UT-HET 113

Probing Models of Dirac Neutrino Masses via the Flavor Structure of the Mass Matrix

Shinya Kanemura,[1,*] Kodai Sakurai,[1,†] and Hiroaki Sugiyama[1,‡]

[1] *Department of Physics, University of Toyama, 3190 Gofuku, Toyama 930-8555, Japan*

arXiv:1603.08679v2 [hep-ph] 25 May 2016

Abstract

We classify models of the Dirac neutrino mass by concentrating on flavor structures of the mass matrix. The advantage of our classification is that we do not need to specify detail of models except for Yukawa interactions because flavor structures can be given only by products of Yukawa matrices. All possible Yukawa interactions between leptons (including the right-handed neutrino) are taken into account by introducing appropriate scalar fields. We also take into account the case with Yukawa interactions of leptons with the dark matter candidate. Then, we see that flavor structures can be classified into seven groups. The result is useful for the efficient test of models of the neutrino mass. One of seven groups can be tested by measuring the absolute neutrino mass. Other two can be tested by probing the violation of the lepton universality in $\ell \to \ell' \nu \overline{\nu}$. In order to test the other four groups, we can rely on searches for new scalar particles at collider experiments.

*Electronic address: kanemu@sci.u-toyama.ac.jp

†Electronic address: sakurai@jodo.sci.u-toyama.ac.jp

‡Electronic address: sugiyama@sci.u-toyama.ac.jp

I. INTRODUCTION

Discoveries of neutrino oscillations [1–9] indicate that neutrinos have tiny but non-zero masses, which is a clear evidence for the new physics beyond the standard model (SM). The SM must be extended to have neutrino masses. There are two possibilities for mass terms of ν_L, which is the left-handed neutrino in an SU(2)$_L$-doublet lepton field $L \equiv (\nu_L \ \ell_L)^T$ with the left-handed charged lepton ℓ_L. One is the Dirac mass term $m_{\rm D}\left[\overline{\nu_L}\nu_R\right]$, for which right-handed neutrino ν_R is introduced as the singlet fermion under the SM gauge group. The other is the Majorana mass term $(1/2)m_{\rm M}\left[\overline{\nu_L}(\nu_L)^c\right]$, where the superscript c denotes the charge conjugation. The Majorana mass term violates the lepton number (L#) conservation by two units. If the Dirac mass term is generated via the Yukawa interaction $y_\nu[\overline{L}\epsilon\Phi^*\nu_R]$ with the Higgs doublet field Φ in the SM, where ϵ denotes 2×2 antisymmetric matrix, the Yukawa coupling constant y_ν must be unnaturally small ($y_\nu \lesssim 10^{-12}$ for $m_{\rm D} \lesssim 0.1\,{\rm eV}$). On the other hand, the Majorana mass term is obtained from dimension-5 operators [10], e.g. $(1/\Lambda)[\overline{L}\epsilon\Phi^*][\Phi^\dagger\epsilon L^c]$, where Λ is the energy scale of the new physics. Then, it seems to be an attractive feature of the Majorana neutrino mass that the mass can be suppressed by a large Λ without using extremely small coupling constants as in the case of the seesaw mechanism [11].

Some of models of the neutrino mass have common features. Classification of models according to such features is useful for the efficient test of models not one by one but group by group of them. The feature that is used for the classification is desired to be model-independent as much as possible. In Ref. [12], it was proposed to classify models for Majorana neutrino masses according to combinations of Yukawa matrices, which give the flavor structure (ratios of elements) of the neutrino mass matrix without specifying detail of models. In contrast, the overall scale of the mass matrix depends on details of models, namely topologies (tree level, one-loop level, etc.) of Feynman diagrams for the mass matrix, sizes of coupling constants in the diagram, and masses of particles in the diagram. Classifications according to topologies of diagrams [13] or higher-dimensional operators [14] are also useful to exhaust possible models.

In Ref. [12], models that generate the Majorana neutrino mass matrix $m_{\rm M}$ were classified into three groups according to combinations of Yukawa matrices. It was shown that these groups can be tested by measurements of the absolute neutrino mass [15, 16], searches for

$\tau \to \overline{\ell_1}\ell_2\ell_3$ ($\ell_1, \ell_2, \ell_3 = e, \mu$) [17], searches for the neutrinoless double beta decay ($0\nu\beta\beta$. See e.g. Ref. [18]), and neutrino oscillation experiments (see e.g. [19]).

In this letter, we classify models for the Dirac neutrino mass matrix $m_{\rm D}$ according to combinations of Yukawa matrices subsequently to the work for the Majorana case in Ref. [12]. The L# conservation is respected because the L# violating phenomena such as $0\nu\beta\beta$ has not been observed so far. New physics models for the Dirac neutrino mass can be found in e.g. Refs. [20–29] (see also Ref. [30]). First, we do the classification for models without new fermions except for ν_R, which has L# = 1. All possible Yukawa interactions between leptons are taken into account by introducing appropriate scalar fields. However, we forbid $y_\nu[\overline{L}\epsilon\Phi^*\nu_R]$ because it requires unnaturally small y_ν. Next, we introduce ψ^0_R as the singlet fermion under the SM gauge group with L# = 0 in order to have the dark matter candidate. We classify models that have additional Yukawa interactions of leptons with ψ^0_R, for which scalar fields are further introduced. As the result of these analyses, we find that these models can be classified into seven groups. We also show how these groups can be tested by $0\nu\beta\beta$ searches, measurements of the absolute neutrino mass, the lepton universality test in $\ell \to \ell'\nu\overline{\nu}$, and neutrino oscillation measurements with/without additional information from future collider experiments.

II. CLASSIFICATION BY FLAVOR STRUCTURES

In this section, we classify models that generate Dirac neutrino masses in order for efficient tests of them. For Dirac neutrino masses, right-handed neutrinos ν_{iR} with L# = 1 must be introduced. The conservation of L# is imposed, which forbids Majorana mass terms $(1/2)M_{iR}\left[\overline{(\nu_{iR})^c}\nu_{iR}\right]$. The index i runs from 1 to 3 in order to obtain three Dirac neutrino masses[1]. If the Dirac neutrino mass is generated via the tree level Yukawa interaction $y_\nu[\overline{L}\epsilon\Phi^*\nu_R]$, the Yukawa coupling constant y_ν must be unnaturally small. Even if we accept such a tiny coupling constant, it makes the origin of the neutrino mass untestable. Therefore, we assume that neutrino masses are generated by a different mechanism. The tree level Yukawa interaction is forbidden by introducing the softly-broken Z_2 symmetry (we call it Z_2') such that ν_R has the odd parity while the SM particles have the even parity[2]. Then,

[1] If one of three neutrino is massless, two ν_{iR} are enough.
[2] Instead of the Z_2' symmetry, we can impose the global $U(1)$ symmetry (see e.g. Ref. [21]).

the Dirac neutrino masses can be generated via the soft-breaking of the Z_2' symmetry. The soft-breaking parameters are assumed to be in the scalar potential, which we do not specify in our model-independent analyses.

Since we classify models according to combinations of Yukawa matrices, we must specify Yukawa matrices that are used in our analyses. First, we take into account all possible Yukawa interactions between leptons (except for the tree level interaction discussed in the previous paragraph). In order to have such interactions, we introduce new scalar fields as listed in Table I. Two scalar fields s_R^+ and Φ_ν are introduced as the Z_2'-odd ones so that they can provide Yukawa interactions between ν_R and leptons. Although we forbid $y_\nu[\overline{L}\epsilon\Phi^*\nu_R]$, the Yukawa interaction $Y_\nu[\overline{L}\epsilon\Phi_\nu^*\nu_R]$ is acceptable because the scale of Y_ν is not necessarily to be extremely small [21, 31][3]. When we introduce Φ_2 in addition to Φ in the SM, another softly-broken Z_2 symmetry is imposed such that only Φ_2 couples with ℓ_R in order to forbid the flavor changing neutral current [33–35]. Then, Φ_2 provides the diagonal Yukawa matrix, whose diagonal elements y_ℓ are proportional to the charged lepton masses m_ℓ. In contrast, s_L^+ gives the antisymmetric Yukawa matrix Y_A^s while s^0, s^{++}, and Δ have symmetric Yukawa matrices Y_S^0, Y_S^s, and Y_S^Δ, respectively. Notice that s^0 and Δ^0 with $\mathrm{L}\# = -2$ must not have the vacuum expectation values because of the lepton number conservation. When ν_L is connected to ν_R by using combinations of the charged current interaction and Yukawa interactions in Table I, these combinations correspond to some models for generating m_D. As long as we concentrate on the flavor structure, it is not necessary to specify how the scalar lines are closed. If we specify that, it gives a certain model.

Each of fermions $(\ell_L, \ell_R, (\ell_L)^c, (\ell_R)^c, (\nu_L)^c, (\nu_R)^c)$ should not be used twice on a fermion line from ν_L to ν_R. If a fermion is used twice on a line, removal of the structure between them gives a simpler line, which is expected to have a larger contribution to m_D. Fermions $(\nu_L)^c$ and $(\nu_R)^c$ must not appear at the same time on the fermion line because the structure between them gives a simpler mechanism to generate m_D. Similarly, when both of ℓ_L and ℓ_R ($(\ell_L)^c$ and $(\ell_R)^c$) exist on a fermion line, they should be next to each other. If there is a structure between them, the replacement of the structure with y_ℓ provides a simpler mechanism, whose contribution to m_D is expected to be larger[4]. One might think that ℓ_L

[3] If the Z_2' is broken not softly but spontaneously [20], the scale of Y_ν is constrained to be extremely small [32].

[4] Since y_ℓ includes $y_\tau \sim 10^{-2}$, the contribution with y_ℓ would not be negligible although $y_e \sim 10^{-6}$ is

should appear next to ν_L because of the charged current interaction. We do not take the restriction because there is a counter example (the Zee model [36]) for the Majorana neutrino mass. However, we see that ℓ_L always appears next to ν_L as a result of our analyses for the Dirac neutrino mass. Assuming that the neutrino mass matrix is generated by a single mechanism (a pattern of alignments of Yukawa matrices), we find there are seven possibilities for the flavor structure as follows:

$$m_{\rm D} \propto Y_A^s \, y_\ell \, Y^s, \tag{1}$$

$$m_{\rm D} \propto Y_S^\Delta \, y_\ell \, Y^s, \tag{2}$$

$$m_{\rm D} \propto y_\ell \, (Y_S^s)^* \, Y^s, \tag{3}$$

$$m_{\rm D} \propto g_2 \, y_\ell \, (Y_S^s)^* \, Y^s, \tag{4}$$

$$m_{\rm D} \propto y_\ell \, (Y^s)^* \, Y_S^0, \tag{5}$$

$$m_{\rm D} \propto g_2 \, y_\ell \, (Y^s)^* \, Y_S^0, \tag{6}$$

$$m_{\rm D} \propto Y_\nu, \tag{7}$$

where g_2 is the $\mathrm{SU}(2)_L$ gauge coupling constant, and Yukawa matrices (Y_A^s, y_ℓ, Y^s, Y_S^Δ, Y_S^s, Y_S^0, Y_ν) are defined in Table I. Diagrams of fermion lines for eqs. (1)-(7) are presented in Figs. 1-7, respectively. Since the charged current interaction does not depend on the flavor, eqs. (3) and (4) (eqs. (5) and (6)) have the same flavor structure. However, eqs. (3) and (4) (eqs. (5) and (6)) correspond to different models because the second Higgs doublet field Φ_2 is required to be introduced for eq. (3) (eq. (5))[5].

The model in Refs. [24, 25] is an example for the structure in Fig. 1. The scalar lines are connected via the interaction $\mu^2[s_L^+ s_R^-]$, where μ is the soft-breaking parameter for Z_2'. For Fig. 7, explicit models can be found in Refs. [20, 21]. The Z_2' symmetry can be softly broken by $\mu^2[\Phi^\dagger \Phi_\nu]$. For the other five structures in Figs. 2-6, explicit models have not been known. In Appendix A, we show an example to close scalar lines for each of Figs. 2-6.

Next, we classify models that have the dark matter candidate. In addition to ν_{iR} and scalar fields in Table I, we introduce ψ_{iR}^0 as singlet fermions under the SM gauge group. The number of ψ_R is equal to or more than 3 in order to obtain three neutrino masses.

rather small.

[5] Although the contribution from eq. (4) (eq. (6)) still exists even if Φ_2 is introduced, it must not be the dominant one unless the fine tuning of parameters. See also Figs. 19 and 20 in Appendix A.

Scalar	$SU(2)_L$	$U(1)_Y$	L#	Z_2'	Yukawa	Note
s^0	$\underline{\mathbf{1}}$	0	-2	Even	$(Y_S^0)_{ij}\left[\overline{(\nu_{iR})^c}\,\nu_{jR}\,s^0\right]$	Symmetric
s_L^+	$\underline{\mathbf{1}}$	1	-2	Even	$(Y_A^s)_{\ell\ell'}\left[\overline{L_\ell}\,\epsilon L_{\ell'}^c\,s_L^-\right]$	Antisymmetric
s_R^+	$\underline{\mathbf{1}}$	1	-2	Odd	$(Y^s)_{\ell i}\left[\overline{(\ell_R)^c}\,\nu_{iR}\,s_R^+\right]$	Arbitrary
s^{++}	$\underline{\mathbf{1}}$	2	-2	Even	$(Y_S^s)_{\ell\ell'}\left[\overline{(\ell_R)^c}\,\ell'_R\,s^{++}\right]$	Symmetric
$\Phi_\nu=\begin{pmatrix}\phi_\nu^+\\ \phi_\nu^0\end{pmatrix}$	$\underline{\mathbf{2}}$	$\frac{1}{2}$	0	Odd	$(Y_\nu)_{\ell i}\left[\overline{L_\ell}\,\epsilon\,\Phi_\nu^*\,\nu_{iR}\right]$	Arbitrary
$\Phi_2=\begin{pmatrix}\phi_2^+\\ \phi_2^0\end{pmatrix}$	$\underline{\mathbf{2}}$	$\frac{1}{2}$	0	Even	$y_\ell\left[\overline{L_\ell}\,\Phi_2\,\ell_R\right]$	Diagonal
$\Delta=\begin{pmatrix}\frac{\Delta^+}{\sqrt{2}} & \Delta^{++}\\ \Delta^0 & -\frac{\Delta^+}{\sqrt{2}}\end{pmatrix}$	$\underline{\mathbf{3}}$	1	-2	Even	$(Y_S^\Delta)_{\ell\ell'}\left[\overline{L_\ell}\,\Delta^\dagger\epsilon\,L_{\ell'}^c\right]$	Symmetric

TABLE I: Scalar fields which have Yukawa interactions with leptons.

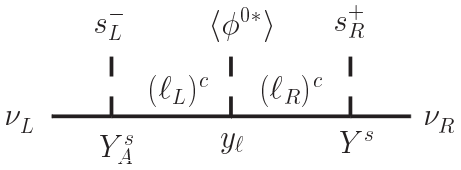

FIG. 1: The diagram for the flavor structure in eq. (1).

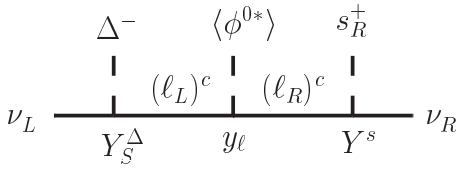

FIG. 2: The diagram for the flavor structure in eq. (2).

The lepton number L# = 0 is assigned to ψ_R^0 in contrast to ν_R with L#=1. The Majorana mass term $(1/2)M_\psi\left[\overline{(\psi_R^0)^c}\psi_R^0\right]$ is not forbidden by the lepton number conservation. For our classification, we use Yukawa interactions between ψ_R^0 and leptons by introducing scalar fields listed in Table II. Representations of s_2^0, s_2^+, and η under the SM gauge group are the same as those of s^0, s_L^+, and Φ (Φ_2), respectively. The scalar fields in Table II have L# = -1 while L# of s^0, s_L^+, and Φ (Φ_2) are even numbers. For concreteness, we take s_2^0 as an odd field under Z_2' while s_2^+, η, and ψ_R^0 are taken as even fields[6]. Notice that there

[6] The opposite assignment is also acceptable.

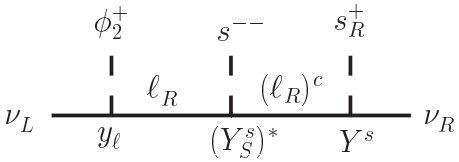

FIG. 3: The diagram for the flavor structure in eq. (3).

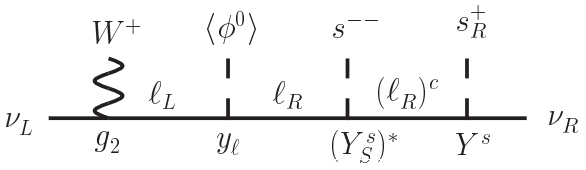

FIG. 4: The diagram for the flavor structure in eq. (4).

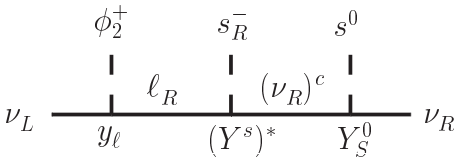

FIG. 5: The diagram for the flavor structure in eq. (5).

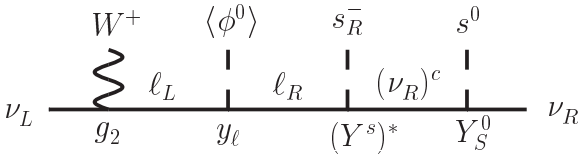

FIG. 6: The diagram for the flavor structure in eq. (6).

appears an unbroken Z_2 symmetry, where ψ_R^0 and scalar fields in Table II are odd due to the L# assignments[7]. Since the lightest Z_2-odd particle is stable, it can be the dark matter candidate (if it is electrically neutral).

Let us consider fermion lines to connect ν_L with ν_R by using also the Z_2-odd particles. Similarly to the case without the Z_2-odd particles, ψ_R^0 and $(\psi_R^0)^c$ should not appear twice on a fermion line. When both of them appear, they should be next to each other because of

[7] The global $U(1)_{F\#+L\#}$ symmetry, where F# denotes the fermion number, is broken down into the Z_2 symmetry by the Majorana mass term of ψ_R^0. Each field has the Z_2 parity $(-1)^{F\#+L\#}$. At the same time, the L# conservation protects the Z_2 breaking because Z_2-odd scalar fields have non-zero L#.

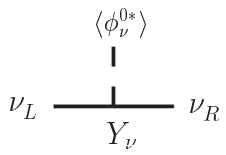

FIG. 7: The diagram for the flavor structure in eq. (7).

their mass term. In addition to eqs. (1)-(7), we obtain the following eleven combinations:

$$m_{\rm D} \propto Y_A^s\, y_\ell\, Y_\psi^+\, M_\psi^{-1}\, (Y_\psi^0)^T, \tag{8}$$

$$m_{\rm D} \propto Y_S^\Delta\, y_\ell\, Y_\psi^+\, M_\psi^{-1}\, (Y_\psi^0)^T, \tag{9}$$

$$m_{\rm D} \propto Y_\psi^\eta\, M_\psi^{-1}\, (Y_\psi^\eta)^T\, y_\ell\, Y^s, \tag{10}$$

$$m_{\rm D} \propto y_\ell\, (Y_\psi^+)^*\, M_\psi^{-1}\, (Y_\psi^+)^\dagger\, Y^s, \tag{11}$$

$$m_{\rm D} \propto g_2\, y_\ell\, (Y_\psi^+)^*\, M_\psi^{-1}\, (Y_\psi^+)^\dagger\, Y^s, \tag{12}$$

$$m_{\rm D} \propto y_\ell\, (Y^s)^*\, Y_\psi^0\, M_\psi^{-1}\, (Y_\psi^0)^T, \tag{13}$$

$$m_{\rm D} \propto g_2\, y_\ell\, (Y^s)^*\, Y_\psi^0\, M_\psi^{-1}\, (Y_\psi^0)^T, \tag{14}$$

$$m_{\rm D} \propto y_\ell\, (Y_\psi^+)^*\, (Y_\psi^0)^T, \tag{15}$$

$$m_{\rm D} \propto g_2\, y_\ell\, (Y_\psi^+)^*\, (Y_\psi^0)^T, \tag{16}$$

$$m_{\rm D} \propto Y_\psi^\eta\, (Y_\psi^+)^\dagger\, Y^s, \tag{17}$$

$$m_{\rm D} \propto Y_\psi^\eta\, M_\psi^{-1}\, (Y_\psi^0)^T, \tag{18}$$

where Yukawa matrices Y_ψ^0, Y_ψ^+, and Y_ψ^η are defined in Table II. Fermion lines for eqs. (8)-(18) are shown in Figs. 8-18. The flavor structures of eqs. (11), (13), and (15) are the same as those of eqs. (12), (14), and (16), respectively. They correspond to different models because eqs. (11), (13), and (15) require Φ_2.

Scalar lines in Fig. 18 can be connected via $\mu[\Phi^\dagger \eta (s_2^0)^*]$ as we see in Ref. [27] (See also Ref. [28]). For the other ten structures in Figs. 8-17, explicit models have not been known. An example to close scalar lines for each of Figs. 8-17 is presented in Appendix B.

As a result, structures in eqs. (1)-(7) and eqs. (8)- (18) can be classified into seven groups

Scalar	$SU(2)_L$	$U(1)_Y$	L#	Z_2'	Yukawa	Note
s_2^0	$\underline{\mathbf{1}}$	0	-1	Odd	$(Y_\psi^0)_{ij}\left[\overline{(\nu_{iR})^c}\,\psi_{jR}^0\,s_2^0\right]$	Arbitrary
s_2^+	$\underline{\mathbf{1}}$	1	-1	Even	$(Y_\psi^+)_{\ell i}\left[\overline{(\ell_R)^c}\,\psi_{iR}^0\,s_2^+\right]$	Arbitrary
$\eta=\begin{pmatrix}\eta^+\\ \eta^0\end{pmatrix}$	$\underline{\mathbf{2}}$	$\frac{1}{2}$	-1	Even	$(Y_\psi^\eta)_{\ell i}\left[\overline{L_\ell}\,\epsilon\,\eta^*\,\psi_{iR}^0\right]$	Arbitrary

TABLE II: Scalar fields which have Yukawa interactions with ψ_R^0 and leptons.

as follows:

$$\text{Group-I}: \ m_{\rm D} \propto Y_A^s\, y_\ell\, X^s, \qquad X^s = Y^s,\ Y_\psi^+\, M_\psi^{-1}\,(Y_\psi^0)^T, \tag{19}$$

$$\text{Group-II}: \ m_{\rm D} \propto X_{SL}\, y_\ell\, X^s,$$

$$\{X_{SL},\ X^s\} = \{Y_S^\Delta,\ Y^s\},\ \{Y_\psi^\eta\, M_\psi^{-1}(Y_\psi^\eta)^T,\ Y^s\},\ \{Y_S^\Delta,\ Y_\psi^+\, M_\psi^{-1}\,(Y_\psi^0)^T\}, \tag{20}$$

$$\text{Group-III}: \ m_{\rm D} \propto y_\ell\, X_{SR}^*\, Y^s, \qquad X_{SR} = Y_S^s,\ (Y_\psi^+)^*\, M_\psi^{-1}\,(Y_\psi^+)^\dagger, \tag{21}$$

$$\text{Group-IV}: \ m_{\rm D} \propto y_\ell\,(Y^s)^*\, X_{S\nu}, \qquad X_{S\nu} = Y_S^0,\ Y_\psi^0\, M_\psi^{-1}\,(Y_\psi^0)^T, \tag{22}$$

$$\text{Group-V}: \ m_{\rm D} \propto y_\ell\, X_\psi, \qquad X_\psi = (Y_\psi^+)^*\,(Y_\psi^0)^T, \tag{23}$$

$$\text{Group-VI}: \ m_{\rm D} \propto X_\psi^\eta\, Y^s, \qquad X_\psi^\eta = Y_\psi^\eta\,(Y_\psi^+)^\dagger, \tag{24}$$

$$\text{Group-VII}: \ m_{\rm D} \propto X_\nu, \qquad X_\nu = Y_\nu,\ (Y_\psi^\eta)\, M_\psi^{-1}\,(Y_\psi^0)^T. \tag{25}$$

Notice that X_{SL}, X_{SR}, and $X_{S\nu}$ are symmetric matrices. Structures of these groups are given in terms of interactions between leptons (new fermions are hidden in interactions X) and cannot be simpler. Therefore, they cannot be included in any other groups, and they correspond to independent models. Models in Refs. [24–26] are included in the Group-I. The Group-VII contains models in Refs. [27–29]. Although the flavor structure in the Dirac seesaw mechanism [22] is the same as the structure of the Group-VII, we do not put it into the group. This is because the Dirac seesaw mechanism has no charged scalar, which contributes to charged lepton decays, unlike models in Refs. [27–29]. Since models in Ref. [23] is given by extending the gauge group of the SM, they are not included in the above seven groups.

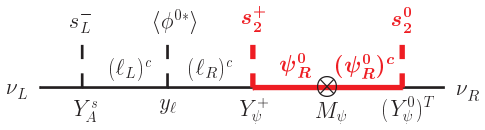

FIG. 8: The diagram for the flavor structure in eq. (8). Bold red lines are for odd particles of the unbroken Z_2 symmetry.

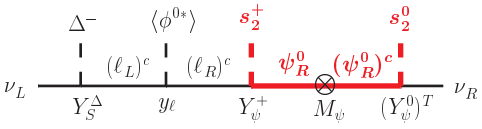

FIG. 9: The diagram for the flavor structure in eq. (9). Bold red lines are for odd particles of the unbroken Z_2 symmetry.

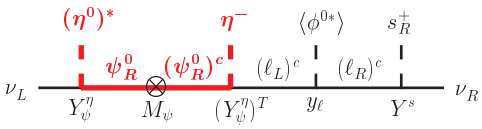

FIG. 10: The diagram for the flavor structure in eq. (10). Bold red lines are for odd particles of the unbroken Z_2 symmetry.

III. DISCUSSION

Let us discuss how we can test these groups in eqs. (19)-(25). The simplest test is the search for $0\nu\beta\beta$, where the conservation of L# is violated by two units. If the decay is observed, all groups in eqs. (19)-(25) will be excluded because they are given by assuming the L# conservation.

By taking the basis where ν_{iR} are mass-eigenstates, the Dirac neutrino mass matrix $m_{\rm D}$ can be expressed as $m_{\rm D} = U_{\rm MNS}\,{\rm diag}(m_1, m_2, m_3)$, where m_i (i = 1-3) are neutrino mass eigenvalues. The case of $m_1 < m_3$ is referred to as the normal mass ordering (NO) while $m_3 < m_1$ is called as the inverted mass ordering (IO). The mixing matrix $U_{\rm MNS}$ is the so-called Maki-Nakagawa-Sakata (MNS) matrix [37], which can be parameterized as

$$U_{\rm MNS} = \begin{pmatrix} 1 & 0 & 0 \\ 0 & c_{23} & s_{23} \\ 0 & -s_{23} & c_{23} \end{pmatrix} \begin{pmatrix} c_{13} & 0 & s_{13}e^{-i\delta} \\ 0 & 1 & 0 \\ -s_{13}e^{i\delta} & 0 & c_{13} \end{pmatrix} \begin{pmatrix} c_{12} & s_{12} & 0 \\ -s_{12} & c_{12} & 0 \\ 0 & 0 & 1 \end{pmatrix}, \tag{26}$$

where $c_{ij} \equiv \cos\theta_{ij}$ and $s_{ij} \equiv \sin\theta_{ij}$. For Group-I ($m_{\rm D} \propto Y_A^s\, y_\ell\, X^s$), we see that ${\rm Det}(m_{\rm D}) \propto {\rm Det}(Y_A) = 0$. Then, the smallest eigenvalue must be zero, namely $m_1 = 0$ or $m_3 = 0$.

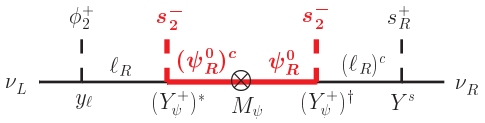

FIG. 11: The diagram for the flavor structure in eq. (11). Bold red lines are for odd particles of the unbroken Z_2 symmetry.

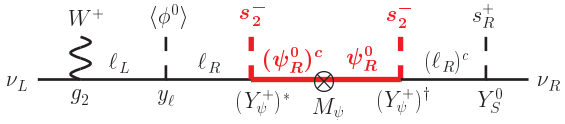

FIG. 12: The diagram for the flavor structure in eq. (12). Bold red lines are for odd particles of the unbroken Z_2 symmetry.

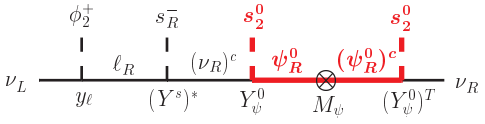

FIG. 13: The diagram for the flavor structure in eq. (13). Bold red lines are for odd particles of the unbroken Z_2 symmetry.

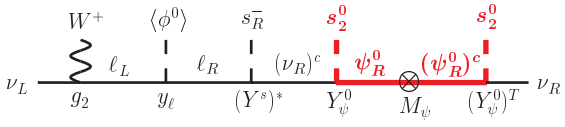

FIG. 14: The diagram for the flavor structure in eq. (14). Bold red lines are for odd particles of the unbroken Z_2 symmetry.

The direct measurement of the absolute neutrino mass can be achieved at the KATRIN experiment [15], whose expected sensitivity is 0.35 eV at 5σ confidence level. The Group-I is excluded if the experiment gives an affirmative result. Cosmological observations put the indirect bound $\sum_i m_i < 0.23\,\text{eV}$ (90 % confidence level) [38], and the future experiments are expected to have the sensitivity to $\sum_i m_i = \mathcal{O}(0.01)\,\text{eV}$ [16]. If $\sum_i m_i \lesssim 0.1\,\text{eV}$ is excluded, we see that the lightest neutrino mass is not zero, and consequently the Group-I is excluded. We have the same conclusion if exclusion of $\sum_i m_i \lesssim 0.06\,\text{eV}$ is achieved in addition to determination of IO in neutrino oscillation experiments [19].

The matrix X_ψ for the Group-V ($m_\text{D} \propto y_\ell\, X_\psi$) gives the four-fermion interaction

$$\mathcal{L}_\text{4-fermi} = \left(\frac{1}{16\pi^2}\right)^n \frac{1}{\Lambda^2}(X_\psi)_{\ell i}(X_\psi^\dagger)_{j\ell'}\left[\overline{\ell_R}\gamma_\mu\nu_{iR}\right]\left[\overline{\nu_{jR}}\gamma^\mu\ell'_R\right], \tag{27}$$

where Λ is the energy scale of the new physics. If we use $X_\psi = (Y_\psi^+)^*(Y_\psi^0)^T$ as an example, the four-fermion interaction is obtained at the one-loop level ($n = 1$). The interaction causes

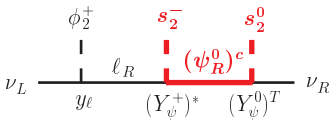

FIG. 15: The diagram for the flavor structure in eq. (15). Bold red lines are for odd particles of the unbroken Z_2 symmetry.

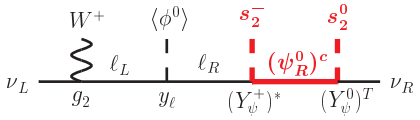

FIG. 16: The diagram for the flavor structure in eq. (16). Bold red lines are for odd particles of the unbroken Z_2 symmetry.

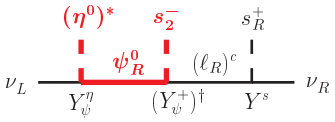

FIG. 17: The diagram for the flavor structure in eq. (17). Bold red lines are for odd particles of the unbroken Z_2 symmetry.

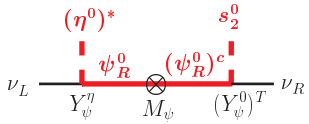

FIG. 18: The diagram for the flavor structure in eq. (18). Bold red lines are for odd particles of the unbroken Z_2 symmetry.

$\ell \to \ell'_R \nu_{iR} \overline{\nu_{jR}}$, which affect to $\ell \to \ell' \nu \overline{\nu}$ in addition to $\ell \to \ell'_L \nu_{\ell L} \overline{\nu_{\ell' L}}$ via the charged current interaction. Since we do not measure neutrino species, contributions from X_ψ are summed up as $(X_\psi X_\psi^\dagger)_{\ell\ell}(X_\psi X_\psi^\dagger)_{\ell'\ell'}$. The Fermi coupling constant G_F is given by measuring $\mu \to e\nu\overline{\nu}$. We have $G_F = G^W \equiv g_2^2/(4\sqrt{2}\, m_W^2)$ in the standard model, where g_2 denotes the $\mathrm{SU}(2)_L$ gauge coupling constant, and m_W is the W boson mass. Although the coupling constants $G_{\tau\ell'}$ $(\ell' = e, \mu)$ given by measuring $\tau \to \ell' \nu \overline{\nu}$ in the standard model is equal to G_F, the deviation from it can exist for the Group-V as

$$G_{\tau\ell'}^2 = G_F^2 + (G_{\tau\ell'}^X)^2 - (G_{\mu e}^X)^2, \quad (G_{\ell\ell'}^X)^2 \equiv \left(\frac{1}{16\pi^2}\right)^{2n} \frac{(m_{\rm D} m_{\rm D}^\dagger)_{\ell\ell}(m_{\rm D} m_{\rm D}^\dagger)_{\ell'\ell'}}{8\,\Lambda^4 C_{\rm loop}^4 m_\ell^2 m_{\ell'}^2}, \tag{28}$$

where $(m_{\rm D})_{\ell i} = C_{\rm loop} m_\ell (X_\psi)_{\ell i}$. Coefficients $(m_{\rm D} m_{\rm D}^\dagger)_{\ell\ell}$ are given by

$$
\begin{aligned}
(m_{\rm D} m_{\rm D}^\dagger)_{ee} &= m_1^2 + c_{13}^2 s_{12}^2 \Delta m_{21}^2 + s_{13}^2 \Delta m_{31}^2 && (29)\\
&= m_1^2 + 7.7 \times 10^{-5}\,{\rm eV}^2, && (30)\\
(m_{\rm D} m_{\rm D}^\dagger)_{\mu\mu} &= m_1^2 + (c_{23}^2 c_{12}^2 + s_{23}^2 s_{13}^2 s_{12}^2 - 2 c_{23} s_{23} s_{13} c_{12} s_{12} \cos\delta) \Delta m_{21}^2 + s_{23}^2 c_{13}^2 \Delta m_{31}^2 && (31)\\
&= m_1^2 + (1.3 \times 10^{-3} - 5.0 \times 10^{-6} \cos\delta)\,{\rm eV}^2, && (32)\\
(m_{\rm D} m_{\rm D}^\dagger)_{\tau\tau} &= m_1^2 + (s_{23}^2 c_{12}^2 + c_{23}^2 s_{13}^2 s_{12}^2 + 2 c_{23} s_{23} s_{13} c_{12} s_{12} \cos\delta) \Delta m_{21}^2 + c_{23}^2 c_{13}^2 \Delta m_{31}^2 && (33)\\
&= m_1^2 + (1.3 \times 10^{-3} + 5.0 \times 10^{-6} \cos\delta)\,{\rm eV}^2 && (34)
\end{aligned}
$$

for NO and

$$
\begin{aligned}
(m_{\rm D} m_{\rm D}^\dagger)_{ee} &= m_3^2 + \Delta m_{13}^2 + c_{13}^2 s_{12}^2 \Delta m_{21}^2 - s_{13}^2 \Delta m_{13}^2 && (35)\\
&= m_3^2 + 2.4 \times 10^{-3}\,{\rm eV}^2, && (36)\\
(m_{\rm D} m_{\rm D}^\dagger)_{\mu\mu} &= m_3^2 + \Delta m_{13}^2 \\
&\quad + (c_{23}^2 c_{12}^2 + s_{23}^2 s_{13}^2 s_{12}^2 - 2 c_{23} s_{23} s_{13} c_{12} s_{12} \cos\delta) \Delta m_{21}^2 - s_{23}^2 c_{13}^2 \Delta m_{13}^2 && (37)\\
&= m_3^2 + (1.2 \times 10^{-3} - 5.0 \times 10^{-6} \cos\delta)\,{\rm eV}^2, && (38)\\
(m_{\rm D} m_{\rm D}^\dagger)_{\tau\tau} &= m_3^2 + \Delta m_{13}^2 \\
&\quad + (s_{23}^2 c_{12}^2 + c_{23}^2 s_{13}^2 s_{12}^2 + 2 c_{23} s_{23} s_{13} c_{12} s_{12} \cos\delta) \Delta m_{21}^2 - c_{23}^2 c_{13}^2 \Delta m_{13}^2 && (39)\\
&= m_3^2 + (1.3 \times 10^{-3} + 5.0 \times 10^{-6} \cos\delta)\,{\rm eV}^2 && (40)
\end{aligned}
$$

for IO. We used the following values:

$$
\begin{aligned}
&|\Delta m_{32}^2| = 2.51 \times 10^{-3}\,{\rm eV}^2\ [6], \quad \Delta m_{21}^2 = 7.46 \times 10^{-5}\,{\rm eV}^2\ [2], && (41)\\
&\sin^2\theta_{23} = 0.514\ [6], \quad \sin^2(2\theta_{13}) = 0.084\ [8], \quad \tan^2\theta_{12} = 0.427\ [2], && (42)
\end{aligned}
$$

where $\Delta m_{ij}^2 \equiv m_i^2 - m_j^2$. We see $(G_{\mu e}^X)^2 \gg (G_{\tau\ell'}^X)^2$ due to $1/(m_\ell^2 m_{\ell'}^2)$, and the Group-V predicts $G_{\tau e}^2 \simeq G_{\tau\mu}^2 \lesssim G_F^2$.

Similarly to the Group-V, the Group-VII ($m_{\rm D} \propto X_\nu$) causes $\ell \to \ell'_L \nu_{iR} \overline{\nu_{jR}}$ via

$$
(G_{\ell\ell'}^X)^2 \equiv \left(\frac{1}{16\pi^2}\right)^{2n} \frac{(m_{\rm D} m_{\rm D}^\dagger)_{\ell\ell} (m_{\rm D} m_{\rm D}^\dagger)_{\ell'\ell'}}{8\,\Lambda^4 v^4 (C'_{\rm loop})^4}, \tag{43}
$$

where $(m_{\rm D})_{\ell i} = C'_{\rm loop}(v/\sqrt{2})(X_\nu)_{\ell i}$. If we take $X_\nu = Y_\nu$ as an example, the four-fermion interaction is generated at the tree level ($n = 0$). This contribution is known for models in Refs. [20, 21], which belong to the Group-VII. We see $(m_{\rm D} m_{\rm D}^\dagger)_{ee} \lesssim (m_{\rm D} m_{\rm D}^\dagger)_{\mu\mu} \simeq (m_{\rm D} m_{\rm D}^\dagger)_{\tau\tau}$

for NO and $(m_{\rm D}m_{\rm D}^\dagger)_{ee} \gtrsim (m_{\rm D}m_{\rm D}^\dagger)_{\mu\mu} \simeq (m_{\rm D}m_{\rm D}^\dagger)_{\tau\tau}$ for IO. Therefore, the Group-VII predicts $G_{\tau\mu}^2 \gtrsim G_{\tau e}^2 \simeq G_F^2$ for NO and $G_{\tau\mu}^2 \lesssim G_{\tau e}^2 \simeq G_F^2$ for IO.

Predictions of $G_{\ell\ell'}^2$ for the Group-V and the Group-VII are summarized in Table III. We do not have predictions for the other five groups though charged scalars in these groups can also contribute to $\ell \to \ell'\nu\overline{\nu}$. Experimental bounds are shown in Ref. [39] as

$$\frac{G_{\tau e}^2}{G_F^2} = 1.0029 \pm 0.0046, \tag{44}$$

$$\frac{G_{\tau\mu}^2}{G_F^2} = 0.981 \pm 0.018. \tag{45}$$

The Babar collaboration [40] gives

$$\frac{G_{\tau\mu}^2}{G_{\tau e}^2} = 1.0036 \pm 0.0020, \tag{46}$$

which results in the world average $G_{\tau\mu}^2/G_{\tau e}^2 = 1.0018 \pm 0.0014$. Since experimental results up to now are consistent with the prediction in the standard model, more precise data (at the Belle experiment or the Belle-II experiment [17]) would be desired to test the Group-V and the Group-VII. If a deviation of $G_{\tau\mu}^2/G_{\tau e}^2$ from unity is discovered as predicted for the Group-VII, the group would be tested further by the determination of the ordering of neutrino masses (NO or IO) in neutrino oscillation experiments [19].

For tests of the remaining four groups, we need discovery of some new scalar particle at collider experiments[8]. In the case of discovery of the doubly charged scalar that decays into a pair of the same-sign charged leptons, the Group-II (see Fig. 2) and the Group-III (see Figs. 3 and 4) would be supported. If experiments discover the charged scalar that dominantly decays into τ, the particle could be identified as ϕ_2^-. Then, the Group-III (see Figs. 3 and 11) and the Group-IV (see Figs. 5 and 13) as well as the Group-V (see Fig. 15) would be preferred. The Group-II (see Fig. 10) and the Group-VI (see Fig. 17) would be supported together with the Group-VII (see Fig. 18) if some scalar that comes from η (odd under the unbroken Z_2) is discovered. Even for the Group-I and the Group-VII, which can be tested without discovery of new particles, measurements of decay patterns of the charged scalar

[8] In general, doublet scalar fields affect the electroweak precision tests. However, their contributions are negligible if we take degenerate masses of the charged and the CP-odd Higgs bosons similarly to the case in the two Higgs doublet models (see e.g. Ref. [41]). Since singlet and triplet scalar fields in our analyses do not have vacuum expectation values, they do not have large contributions to the electroweak precision tests.

	Group-V	Group-VII
$\ell \to \ell' \nu \overline{\nu}$	$G^2_{\tau\mu} \simeq G^2_{\tau e} \lesssim G^2_F$	$G^2_{\tau\mu} \gtrsim G^2_{\tau e} \simeq G^2_F$ $(m_1 < m_3)$
		$G^2_{\tau\mu} \lesssim G^2_{\tau e} \simeq G^2_F$ $(m_1 > m_3)$

TABLE III: Predictions for deviations from the lepton universality in cases of the Group-V and the Group-VII.

can be utilized for the test because explicit models for these groups have predictions for the decay patterns [21, 25].

IV. CONCLUSION

In this letter, we have classified new physics models for the Dirac neutrino mass according to combinations of Yukawa interactions. Detail of models is not required for our classification because we concentrate on the flavor structure of the neutrino mass matrix, which is determined only by Yukawa matrices. If all possible Yukawa interactions between leptons are taken into account for our classification, we have found that there are seven combinations of them for the flavor structure of $m_{\rm D}$. Additional eleven combination of Yukawa interactions appear if we add singlet-fermions ψ^0_{iR} with L# = 0 and scalar fields for Yukawa interactions between ψ^0_{iR} and leptons in order to obtain the dark matter candidate. The dark matter candidate is stabilized by the unbroken Z_2 symmetry, which appears due to assignments of L#. We have shown that these combinations can be classified into seven groups.

If the neutrinoless double beta decay is observed, these groups are excluded because the conservation of L#is assumed. The Group-I ($m_{\rm D} \propto Y^s_A\, y_\ell\, X^s$) in eq. (19), where Y^s_A is an antisymmetric Yukawa matrix, predicts $\min(m_1, m_3) = 0$. Thus, the Group-I can be tested by direct [15] and indirect [16] measurements of the absolute neutrino mass. The Group-V ($m_{\rm D} \propto y_\ell\, X_\psi$) in eq. (23), where y_ℓ is the diagonal Yukawa matrix for charged lepton masses, predicts $G^2_{\tau\mu} \simeq G^2_{\tau e} \lesssim G^2_F$ for possible deviations from the lepton universality in $\ell \to \ell' \nu \overline{\nu}$ due to the interaction with the matrix X_ψ. The Group-VII ($m_{\rm D} \propto X_\nu$) in eq. (25) predicts $G^2_{\tau\mu} \gtrsim G^2_{\tau e} \simeq G^2_F$ for $m_1 < m_3$ and $G^2_{\tau\mu} \lesssim G^2_{\tau e} \simeq G^2_F$ for $m_1 > m_3$ via the interaction with the matrix X_ν. Therefore, the Group-V and the Group-VII could be tested at the Belle experiment or the Belle-II experiment [17]. The other four groups can be tested

Scalar	$SU(2)_L$	$U(1)_Y$	L#
s_3^+	$\underline{\mathbf{1}}$	1	0
Φ_3	$\underline{\mathbf{2}}$	$\frac{1}{2}$	-2
Φ_4	$\underline{\mathbf{2}}$	$\frac{3}{2}$	-2

TABLE IV: Examples of scalar fields that can be used to close scalar lines in Figs. 1-6 and Figs. 8-18.

if some scalar particle is discovered at collider experiments. In this way, our classification is useful to discriminate mechanisms for generating Dirac neutrino masses by testing not each model but each group of models.

Acknowledgments

This work was supported, in part, by Grant-in-Aid for Scientific Research No. 23104006 (SK) and Grant H2020-MSCA-RISE-2014 No. 645722 (Non Minimal Higgs) (SK).

Appendix A: Examples to close scalar lines in cases without dark matter

We show examples to close scalar lines for Figs. 1-6 by using additional scalar fields in Table. IV. Notice that these scalar fields do not have Yukawa interactions. In Table V, we summarize scalar particles and relevant interactions for each of Figs. 1-6. See also Figs. 19 and 20.

For Fig. 1, the example corresponds to the model in Refs. [24, 25]. The Z_2' symmetry is softly broken by μ^2. For the other five figures listed in Table V, the parameter μ or μ' softly breaks Z_2' whether the additional scalar is the Z_2'-even or odd. Therefore, we can confirm that both of μ and μ' are necessary to close the scalar line with the soft-breaking of Z_2'. For Fig. 7, which has only a scalar line, explicit models can be found in Refs. [20, 21].

	Scalar	Relevant interaction
Fig. 1	None	$\mu^2[s_L^+ s_R^-]$
Fig. 2	Φ_3	$\mu[\Phi_3^T \epsilon \Phi s_R^-]$, $\mu'[\Phi^\dagger \Delta \epsilon \Phi_3^*]$
Fig. 3	s_3^+	$\mu[s_R^- s^{++} s_3^-]$, $\mu'[\Phi_2^\dagger \epsilon \Phi^* s_3^+]$
Fig. 4	Φ_4	$\mu[\Phi^\dagger \Phi_4 s_R^-]$, $\mu'[\Phi_4^\dagger \epsilon \Phi^* s^{++}]$
Fig. 5	s_3^+	$\mu[s^{0*} s_R^+ s_3^-]$, $\mu'[\Phi_2^\dagger \epsilon \Phi^* s_3^+]$
Fig. 6	Φ_3	$\mu[\Phi_3^\dagger \epsilon \Phi^* s_R^+]$, $\mu'[\Phi^\dagger \Phi_3 (s^0)^*]$

TABLE V: Examples of additional scalar fields and their interactions to close scalar lines of Figs. 1-6.

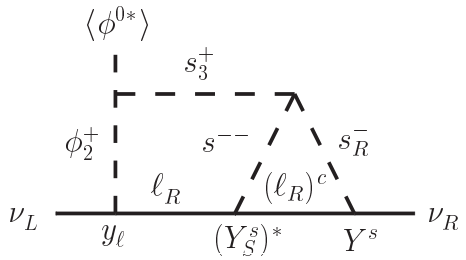

FIG. 19: An example to close scalar lines of the diagram in Fig. 3.

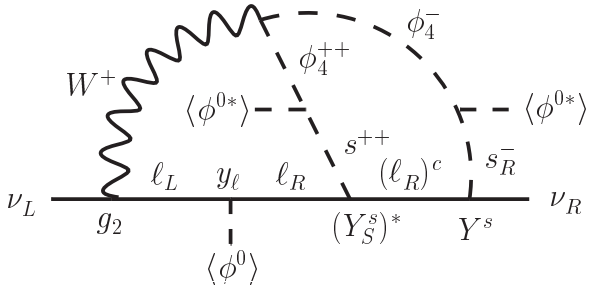

FIG. 20: An example to close scalar lines of the diagram in Fig. 4.

Appendix B: Examples to close scalar lines in cases with dark matter

We show examples to close scalar lines for Figs. 8-18 by using additional scalar fields in Table. IV. In Table VI, we summarize scalar particles and relevant interactions for each of Figs. 8-18.

For Figs. 8 and 18, scalar lines can be simply connected without introducing additional scalar fields, and the Z_2' symmetry is softly broken by the parameter μ. An explicit model for the structure in Fig. 18 can be found in Ref. [27] (See also Ref. [28]). For Figs. 9-14, the parameter μ softly breaks Z_2' when we fix the Z_2' parity for the additional scalar field as shown in Table VI. Since the Z_2' parity for the scalar field is fixed by λ so that the term does not break Z_2', the dimensionless coupling constant λ is also necessary for the soft-breaking of Z_2'. For Figs. 15 and 17, the product $\mu\mu'$ softly breaks Z_2' independently on the Z_2'

	Scalar	Relevant interaction
Fig. 8	None	$\mu[s_L^+ s_2^- (s_2^0)^*]$
Fig. 9	Φ_3 (Z_2'-odd)	$\mu[\Phi^T \Delta \epsilon \Phi_3^*]$, $\lambda[\Phi_3^T \epsilon \Phi s_2^- (s_2^0)^*]$
Fig. 10	Φ_3 (Z_2'-even)	$\mu[\Phi_3^T \epsilon \Phi s_R^-]$, $\lambda[(\Phi^\dagger \eta)(\Phi_3^\dagger \eta)]$
Fig. 11	s_3^+ (Z_2'-odd)	$\mu[\Phi_2^\dagger \epsilon \Phi^* s_3^+]$, $\lambda[s_3^- s_R^- s_2^+ s_2^+]$
Fig. 12	Φ_4 (Z_2'-even)	$\mu[\Phi^\dagger \Phi_4 s_R^-]$, $\lambda[\Phi_4^\dagger \epsilon \Phi^* s_2^+ s_2^+]$
Fig. 13	s_3^+ (Z_2'-odd)	$\mu[\Phi_2^\dagger \epsilon \Phi^* s_3^+]$, $\lambda[(s_2^0)^* (s_2^0)^* s_R^+ s_3^-]$
Fig. 14	Φ_3 (Z_2'-even)	$\mu[\Phi_3^\dagger \epsilon \Phi^* s_R^+]$, $\lambda[\Phi^\dagger \Phi_3 (s_2^0)^* (s_2^0)^*]$
Fig. 15	s_3^+	$\mu[\Phi_2^\dagger \epsilon \Phi^* s_3^+]$, $\mu'[s_3^- s_2^+ (s_2^0)^*]$
Fig. 16	$(s_3^0)^*$, s_3^+ , Φ_3 (Z_2-odd, unbroken)	$\mu[\Phi^\dagger \Phi_3 s_3^0]$, $\mu'[\Phi_3^\dagger \epsilon \Phi^* s_3^+]$, $\lambda[(s_3^0)^* s_3^- (s_2^0)^* s_2^+]$
Fig. 17	Φ_4	$\mu[\Phi_4^\dagger \eta s_2^+]$, $\mu'[\Phi^\dagger \Phi_4 s_R^-]$
Fig. 18	None	$\mu[\Phi^\dagger \eta (s_2^0)^*]$

TABLE VI: Examples of additional scalar fields and their interactions to close scalar lines of Figs. 8-18. For Fig. 16, a common L# is assigned to these additional scalar fields, where s_3^0 is a gauge singlet field. Then, an unbroken Z_2 symmetry is imposed such that these scalar fields have the odd parity.

parity of the additional scalar. For Fig. 16, the scalar lines can be closed by introducing $(s_3^0)^*$ ($\mathrm{SU}(2)_L$-singlet with $Y = 0$) in addition to s_3^+ and Φ_3. Their lepton numbers are common and arbitrary. We additionally impose an unbroken Z_2 symmetry, under which these three scalar fields have the odd parity. We see that the Z_2' symmetry is softly broken by the product $\lambda\mu\mu'$ independently on the Z_2' parities of $(s_3^0)^*$, s_3^+, and Φ_3.

We obtain predictions for the violation of the lepton universality as shown in Table III by concentrating on the flavor structure. If we specify the scalar sector, it is possible to perform further calculations. For example, if scalar lines in Fig. 15 of the Group-V are closed by using s_3^+, we have

$$(G^X_{\ell\ell'})^2 = \left(\frac{1}{16\pi^2}\right)^2 \frac{(m_{\rm D} m_{\rm D}^\dagger)_{\ell\ell} (m_{\rm D} m_{\rm D}^\dagger)_{\ell'\ell'}}{8\,\Lambda^4 C_{\rm loop}^4 m_\ell^2 m_{\ell'}^2}, \quad C_{\rm loop} = \left(\frac{1}{16\pi^2}\right)^2 \frac{\mu\mu'}{\Lambda^2} \tag{B1}$$

By taking $(G^X_{e\mu}/G_F)^2 = 10^{-3}$ with $m_{\rm D} = 0.1\,\mathrm{eV}$ for example, we see $\mu\mu'/\Lambda = \mathcal{O}(10^{-2})\,\mathrm{GeV}$.

[1] B. T. Cleveland, T. Daily, R. Davis, Jr., J. R. Distel, K. Lande, C. K. Lee, P. S. Wildenhain and J. Ullman, Astrophys. J. **496**, 505 (1998); W. Hampel *et al.* [GALLEX Collaboration], Phys. Lett. B **447**, 127 (1999); J. N. Abdurashitov *et al.* [SAGE Collaboration], Phys. Rev. C **80**, 015807 (2009); K. Abe *et al.* [Super-Kamiokande Collaboration], Phys. Rev. D **83**, 052010 (2011); G. Bellini *et al.* [Borexino Collaboration], Phys. Rev. D **89**, no. 11, 112007 (2014).

[2] B. Aharmim *et al.* [SNO Collaboration], Phys. Rev. C **88**, no. 2, 025501 (2013).

[3] A. Gando *et al.* [KamLAND Collaboration], Phys. Rev. D **88**, no. 3, 033001 (2013).

[4] R. Wendell *et al.* [Super-Kamiokande Collaboration], Phys. Rev. D **81**, 092004 (2010).

[5] P. Adamson *et al.* [MINOS Collaboration], Phys. Rev. Lett. **112**, 191801 (2014); P. Adamson *et al.* [NOvA Collaboration], arXiv:1601.05037 [hep-ex].

[6] K. Abe *et al.* [T2K Collaboration], Phys. Rev. D **91**, no. 7, 072010 (2015).

[7] Y. Abe *et al.* [Double Chooz Collaboration], JHEP **1410**, 086 (2014) Erratum: [JHEP **1502**, 074 (2015)]; J. H. Choi *et al.* [RENO Collaboration], arXiv:1511.05849 [hep-ex].

[8] F. P. An *et al.* [Daya Bay Collaboration], Phys. Rev. Lett. **115**, no. 11, 111802 (2015).

[9] K. Abe *et al.* [T2K Collaboration], Phys. Rev. Lett. **112**, 061802 (2014).

[10] S. Weinberg, Phys. Rev. Lett. **43**, 1566 (1979).

[11] P. Minkowski, Phys. Lett. B **67**, 421 (1977); T. Yanagida, Conf. Proc. C **7902131**, 95 (1979); Prog. Theor. Phys. **64**, 1103 (1980); M. Gell-Mann, P. Ramond and R. Slansky, Conf. Proc. C **790927**, 315 (1979); R. N. Mohapatra and G. Senjanovic, Phys. Rev. Lett. **44**, 912 (1980).

[12] S. Kanemura and H. Sugiyama, Phys. Lett. B **753**, 161 (2016).

[13] E. Ma, Phys. Rev. Lett. **81**, 1171 (1998); F. Bonnet, M. Hirsch, T. Ota and W. Winter, JHEP **1207**, 153 (2012); D. Aristizabal Sierra, A. Degee, L. Dorame and M. Hirsch, JHEP **1503**, 040 (2015).

[14] K. S. Babu and C. N. Leung, Nucl. Phys. B **619**, 667 (2001); F. Bonnet, D. Hernandez, T. Ota and W. Winter, JHEP **0910**, 076 (2009); S. Kanemura and T. Ota, Phys. Lett. B **694**, 233 (2011).

[15] A. Osipowicz *et al.* [KATRIN Collaboration], hep-ex/0109033.

[16] K. N. Abazajian *et al.* [Topical Conveners: K.N. Abazajian, J.E. Carlstrom, A.T. Lee Collaboration], Astropart. Phys. **63**, 66 (2015).

[17] T. Abe *et al.* [Belle-II Collaboration], arXiv:1011.0352 [physics.ins-det].

[18] S. Dell'Oro, S. Marcocci, M. Viel and F. Vissani, arXiv:1601.07512 [hep-ph].

[19] M. Blennow, P. Coloma, P. Huber and T. Schwetz, JHEP **1403**, 028 (2014).

[20] F. Wang, W. Wang and J. M. Yang, Europhys. Lett. **76**, 388 (2006); S. Gabriel and S. Nandi, Phys. Lett. B **655**, 141 (2007).

[21] S. M. Davidson and H. E. Logan, Phys. Rev. D **80**, 095008 (2009).

[22] M. Roncadelli and D. Wyler, Phys. Lett. B **133**, 325 (1983); P. Roy and O. U. Shanker, Phys. Rev. Lett. **52**, 713 (1984) Erratum: [Phys. Rev. Lett. **52**, 2190 (1984)].

[23] D. Chang, R. N. Mohapatra, Phys. Rev. Lett. **58**, 1600 (1987); R. N. Mohapatra, Phys. Lett. **B198**, 69 (1987); Phys. Lett. **B201**, 517 (1988); B. S. Balakrishna, R. N. Mohapatra, Phys. Lett. **B216**, 349 (1989); E. Ma, Phys. Rev. Lett. **63**, 1042 (1989); K. S. Babu and X. G. He, Mod. Phys. Lett. A **4**, 61 (1989).

[24] S. Nasri and S. Moussa, Mod. Phys. Lett. A **17**, 771 (2002).

[25] S. Kanemura, T. Nabeshima and H. Sugiyama, Phys. Lett. B **703**, 66 (2011).

[26] C. S. Chen and L. H. Tsai, Phys. Rev. D **88**, no. 5, 055015 (2013).

[27] P. H. Gu and U. Sarkar, Phys. Rev. D **77**, 105031 (2008).

[28] Y. Farzan and E. Ma, Phys. Rev. D **86**, 033007 (2012).

[29] H. Okada, arXiv:1404.0280 [hep-ph].

[30] K. S. Babu and E. Ma, Mod. Phys. Lett. A **4**, 1975 (1989).

[31] S. Kanemura, T. Matsui and H. Sugiyama, Phys. Lett. B **727**, 151 (2013).

[32] S. Zhou, Phys. Rev. D **84**, 038701 (2011); P. A. N. Machado, Y. F. Perez, O. Sumensari, Z. Tabrizi and R. Z. Funchal, JHEP **1512**, 160 (2015).

[33] S. L. Glashow and S. Weinberg, Phys. Rev. D **15**, 1958 (1977).

[34] V. D. Barger, J. L. Hewett and R. J. N. Phillips, Phys. Rev. D **41**, 3421 (1990).

[35] M. Aoki, S. Kanemura, K. Tsumura and K. Yagyu, Phys. Rev. D **80**, 015017 (2009); S. Su and B. Thomas, Phys. Rev. D **79**, 095014 (2009); H. E. Logan and D. MacLennan, Phys. Rev. D **79**, 115022 (2009).

[36] A. Zee, Phys. Lett. B **93**, 389 (1980) Erratum: [Phys. Lett. B **95**, 461 (1980)].

[37] Z. Maki, M. Nakagawa and S. Sakata, Prog. Theor. Phys. **28**, 870 (1962).

[38] P. A. R. Ade *et al.* [Planck Collaboration], arXiv:1502.01589 [astro-ph.CO].

[39] K. A. Olive *et al.* [Particle Data Group Collaboration], Chin. Phys. C **38**, 090001 (2014).

[40] B. Aubert *et al.* [BaBar Collaboration], Phys. Rev. Lett. **105**, 051602 (2010).

[41] S. Kanemura, Y. Okada, H. Taniguchi and K. Tsumura, Phys. Lett. B **704**, 303 (2011).